

Evaluation of Coal Ash–Based CLSM Made with Cementless Binder as a Thermal Grout for Borehole Heat Exchangers

Tan Manh Do¹; Gyeong-O Kang²; Gyu-Hyun Go³; and Young-Sang Kim⁴

Abstract: The primary goal of this study is to assess the characteristics of coal ash–based controlled low-strength material (CLSM) mixtures made with a cementless binder for the feasible usage as a thermal grout in borehole heat exchangers. In the experimental program, a group of CLSM mixtures made with cement or cementless binder through various ratios of water to binder (W:B) and water to solid (W:S). The general properties (e.g., fresh density, flowability, initial setting time, bleeding, unconfined compressive strength, and microstructural analysis), and environmental impacts (e.g., corrosivity and heavy metals) were carried out on CLSM mixtures. Afterward, thermal conductivity was determined following a current specification for verification of the proposed CLSM, which is feasibly used as a thermal grout in geothermal systems (borehole heat exchangers). According to the results, all of the engineering properties and environmental impacts satisfied the specifications of CLSM. In addition, compared with the thermal conductivity values of conventional grouts, those of the proposed CLSM mixtures were higher. In conclusion, owing to good flowability and higher thermal conductivity than conventional grouts, the CLSMs made with cementless binder can be feasibly employed as a thermal grout for borehole heat exchangers. DOI: 10.1061/(ASCE)MT.1943-5533.0002691. © 2019 American Society of Civil Engineers.

Author keywords: Controlled low-strength material (CLSM); Coal ash; Cementless binder; Thermal grout; Borehole heat exchangers.

Introduction

A significant amount of energy is generally required to maintain a comfortable temperature inside a building. In general, electricity, fossil fuels, or biomass are used for the maintenance of the required energy in heating and cooling systems. As reported by the Korea Energy Management Corporation (KEMCO 2006), about 97% of fossil fuel used in Korea was imported from foreign countries. Therefore, renewable energy is indispensable for Korea in the near future. Based on the standpoint that ground-source heat pump (GSHP) systems can transform a geothermal source into renewable energy in the heating and cooling systems of residential homes, the evolution of these systems has been forward-thinking in Korea. In addition, using these systems can save huge amounts of energy compared with conventional air-conditioning systems.

Vertical GSHP systems use the ground as the heat source for the heat interchanger. Thermal grout in this system works as the heat-transfer medium, which is a connection layer between the heat exchanger and soil or rock surrounding the boreholes. In general,

the heat exchange between ground and pipes fluid is significantly affected by the thermal conductivity of the grout. Therefore, the key parameter in this system is the thermal conductivity, which would determine the efficiency of the installation. The schematic of thermal grout in the geothermal system is shown in Fig. 1.

There have been a number of cementitious grouts developed for this system. Initially, bentonite-based grouts were conventionally used as a grout filled in boreholes of geothermal systems (Eckhart 1991). However, the thermal conductivity of these grouts was fairly low (below 0.90 W/m · K) (Remund and Lund 1993), which leads to high heat exchanger lengths. Increasing this thermal conductivity permits an improvement in the heat transfer between soil ground and borehole, thus reducing the heat exchanger length. Even though thermal conductivity is improved by incorporation of filler materials such as silica sand, Axilat, and graphite (Chantal 2016), these bentonite-based grouts are still subject to shrinkage, cracking due to moisture losses, and desiccation (Allan 1997; Philippopoulos and Berndt 2001).

For that reason, a new grout development for borehole heat exchangers in GSHP systems was addressed in many studies. Among these, Allan (1997) developed cement-sand grouts focusing on thermal conductivity and pumpability requirements. The thermal conductivity of these developed cement-sand grouts was higher than that of neat cement or bentonite grouts. Subsequently, Allan and Kavanaugh (1999) successively developed cementitious grouts with different thermally conductive fillers such as alumina, silica sand, steel grit, steel fibers, and silicon carbide. As their obtained results using the aforementioned fillers, the thermal conductivity boosted up to the range of 1.7–3.3 W/(m · K). Allan and Kavanaugh (1999), Xu and Chung (2000), Park et al. (2011), and Lee (2012) all mentioned the overall applicability of cement-based grouts in GSHP systems. Besides, from the standpoint of sustainable development, industrial by-product–based grouts have also been investigated recently.

¹Lecturer, Dept. of Civil Engineering, Hanoi Univ. of Mining and Geology, Hanoi, Vietnam; Former Graduate Student, Dept. of Civil and Environmental Engineering, Chonnam National Univ., Yeosu 59626, Republic of Korea.

²Research Professor, Dept. of Civil and Environmental Engineering, Chonnam National Univ., Yeosu 59626, Republic of Korea.

³Assistant Professor, Dept. of Civil Engineering, Kumoh National Institute of Technology, Gyeongsbuk 39177, Republic of Korea.

⁴Professor, Dept. of Civil Engineering, Chonnam National Univ., Gwangju 61186, Republic of Korea (corresponding author). Email: geoyoungkim@jnu.ac.kr

Note. This manuscript was submitted on March 11, 2018; approved on November 8, 2018; published online on March 26, 2019. Discussion period open until August 26, 2019; separate discussions must be submitted for individual papers. This paper is part of the *Journal of Materials in Civil Engineering*, © ASCE, ISSN 0899-1561.

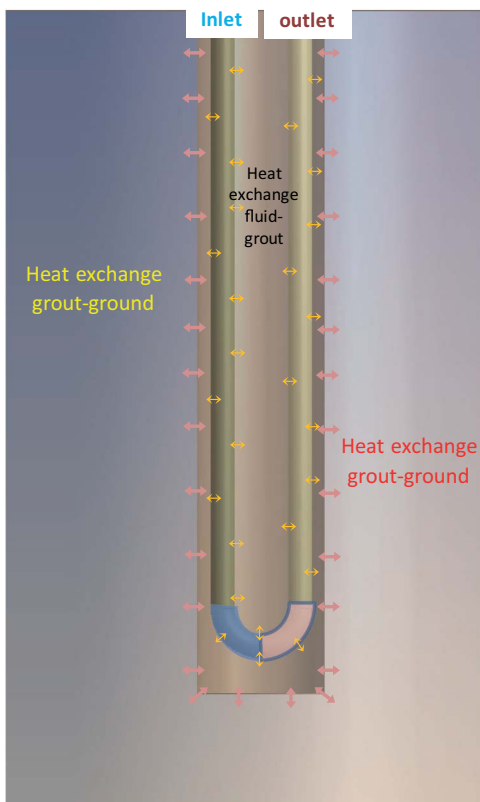


Fig. 1. Schematic of thermal grout in geothermal system.

In the study by Alrtimi et al. (2013), pulverized fuel ash (PFA), owing to good flowability and low shrinkage, was employed to make PFA-based grouts for borehole heat exchangers. The thermal conductivity of their developed grouts was measured at both dry and saturated states. They found that the PFA-based grouts that used fluorspar or coarse sand at 20% of PFA showed the highest thermal conductivity values. Another finding was that the thermal conductivity of PFA-based grouts made with coarse ground glass and fluorspar was acceptable, regardless of grout states (relatively high in both dry and saturated states).

As reported by the American Concrete Institute (ACI) in ACI 229R (ACI 1999), controlled low-strength materials (CLSMs) also have similar aspects (very good workability and low shrinkage) as PFA-based grouts. Nevertheless, no previous research has mentioned the possible use of CLSM in geothermal systems (thermal grout for borehole heat exchangers). Therefore, it is novel to employ CLSM as a backfill (thermal grout) in boreholes of geothermal systems to replace conventional grouts. As defined by the ACI, CLSM is a cementitious material with self-leveling, self-compacting characteristics. Owing to a low unconfined compressive strength, CLSM is largely used to substitute the compacted fill or landfill (Du et al. 2002) or backfill for pipeline alignment (Chittoori et al. 2013; Puppala et al. 2014).

In the meantime, large amounts of coal ash (i.e., a common by-product) are produced every year from thermal power plants (combustion process) in Korea (Jeolla Province). In general, three types of coal ash (fly ash, bottom ash, and ponded ash) are generated from thermal power plants (Bera et al. 2007). Bottom ash is a collection of ash at the bottom of the boilers, and fly ash is assembled by automatic depositors from flue gasses in the top of power plants. Ponded ash is generated when bottom ash and fly ash are mixed together and conveyed in the form of a slurry and finally poured in ponds. Compared with the volume of fly ash or bottom

ash, that of ponded ash is enormous. Problems associated with waste products, such as disposal and leaching, will become serious in the near future. Interestingly, it is possible to reuse coal ash as the mixture components for the production of CLSM [ACI 229R (ACI 1999)].

The present study aims to investigate the feasibility of using CLSM as a thermal grout for borehole heat exchangers by assessing its engineering properties, environmental impacts, and especially thermal conductivity properties considered for a reduction in loop installation costs and finally help to enhance the heat pump coefficient of performance. In addition, the production of cement is connected with the emission of greenhouse gasses such as CO_2 , SO_x , and NO_x . Meanwhile, Korea ranks in the top 10 in the list of countries by carbon dioxide emissions from the burning of fossil fuels and cement manufacture (Do et al. 2018). For that reason, the development of cementless binder using by-products is necessary and encouraged. Using industrial by-products in cementless binder could not only reduce the natural raw materials (coal, limestone, and clay), and energy (electricity) but also eliminate the emission of greenhouse gasses and other toxic pollutants. Therefore, this study investigated the possibility of making CLSM without using cement. CLSM was produced using coal ash (fly ash and ponded ash) and a cementless binder (as a full replacement of cement).

Experimental Investigation

Materials

In general, CLSM mixture consists of fine aggregates, fly ash, portland cement, and water [ACI 229R (ACI 1999)]. Fine aggregate used in the production of CLSM was ponded ash, which comes from cogeneration plants in Jeolla-do Province, Korea. Ponded ash used is a combined mixture of fly ash and bottom ash. These types of ashes produced in the boiler and partially desulfurized are mixed together without being recycled, then conveyed in the form of slurry, and finally poured in ponds. Ponded ash was first subjected to the temperature of 105°C to dry and then sieved through a 9.52-mm sieve to get the particle size of natural fine aggregates (i.e., get rid of unnecessary large particles). The chemical compositions and physical characteristics of ponded ash are tabulated in Tables 1 and 2, respectively. Fig. 2 illustrates the grain-size distribution curve of ponded ash. Based on ASTM D2487 (ASTM 2017a), ponded ash having classification parameters of coefficient of curvature C_c (0.94) and coefficient of uniformity C_u (20.25) is classified as poorly graded sand (Table 3).

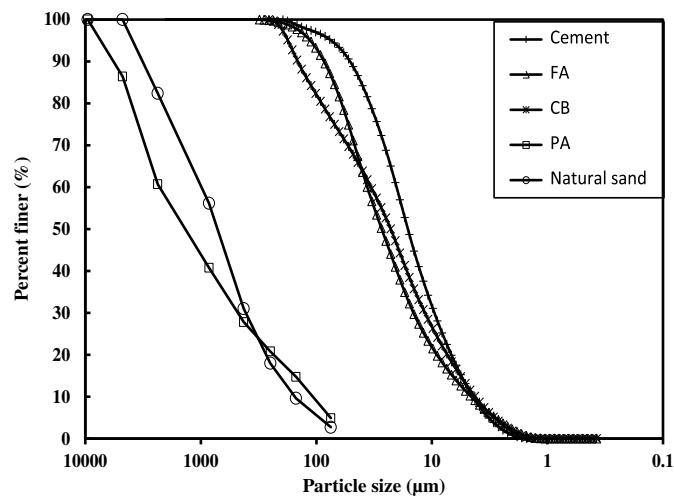
Apart from fine aggregate, factors such as binders or cementitious materials and water also play a key role in CLSM. They help CLSM to harden and gain strength through the hydration process (Do et al. 2015). In the present study, all properties of CLSM made with a cementless binder (CB) were determined and evaluated by comparison with those of CLSM made with cement. Portland cement Type I, which conforms to ASTM C150 (ASTM 2004), was first used in the production of CLSM. Afterwards, cement in CLSM was fully replaced by a cementless binder. The cementless binder used in the experimental program is a nonsintering cement derived from waste lime, phosphogypsum, and granulated blast-furnace slag. In this cementless binder, waste lime and phosphogypsum work as alkali activators and sulfate, respectively (Mun et al. 2007). Fly ash, owing to its spherical-shaped particles, can be used in CLSM for an improvement in the fluidity or flowability of mixtures. In this study, fly ash originating from a thermal power plant in Jeolla Province was used.

Table 1. Chemical composition of ponded ash, fly ash, cement, and cementless binder by weight

Compound	Ponded ash (PA) (%)	Fly ash (FA) (%)	Cement (%)	Cementless binder (CB) (%)
CaO	1.80	1.99	64.35	52.87
SiO ₂	62.53	56.88	17.16	23.57
Al ₂ O ₃	20.91	21.52	3.57	8.72
SO ₃	—	—	2.20	5.70
MgO	0.69	0.92	2.66	2.80
Fe ₂ O ₃	8.70	6.34	4.03	0.56
TiO ₂	1.28	1.21	0.29	0.54
K ₂ O	1.44	1.58	1.11	0.48
Na ₂ O	0.39	0.49	—	0.27
MnO	0.09	0.06	0.20	0.23
P ₂ O ₅	—	—	0.14	—
ZnO	0.01	0.03	0.17	—
Loss of ignition	1.85	8.73	3.93	3.87

Table 2. Physical properties of ponded ash

Property	Value
Maximum dry density (kg/m ³)	1,279
Optimum moisture content (OMC) (%)	17
Natural water content (%)	15.57
Specific gravity	2.15
Water absorption (%)	4.65
Fineness modulus	3.37
Particles <75 μm (%)	4.91
Color	Black

**Fig. 2.** Particle-size distribution of raw materials.

All particle-size distribution curves for raw materials (e.g., cement, cementless binder, ponded ash, and fly ash) are shown in Fig. 2. It can be observed that the particle size of cement and fly ash was rather smaller than that of cementless binder. The X-ray diffraction (XRD) of cementless binder, cement, ponded ash, and fly ash is displayed in Fig. 3. From the results obtained by the XRD patterns, numerous peaks of quartz and mullite in both ponded ash and fly ash (peaks of ponded ash and fly ash were fairly identical) were found. Fig. 3 shows the XRD result of cement, which is well-known. Finally, several components such as lime (free CaO), alite, gypsum, calcite, and some amount of kaolinite were observed in

Table 3. Soil classification parameters for ponded ash

Parameter	Value
D ₁₀ (mm)	0.11
D ₃₀ (mm)	0.49
D ₆₀ (mm)	2.30
C _u	20.25
C _c	0.94
Fineness modulus	3.37
USCS	SP

Note: C_c = coefficient of curvature; C_u = coefficient of uniformity; D₁₀, D₃₀, and D₆₀ = particle diameter such that 10%, 60%, and 30%, respectively, of the soil grain are smaller than this size; SP = poorly graded sand; and USCS = unified soil classification system.

the XRD (X-ray Diffraction) result of cementless binder. SEM (Scanning Electron Microscope) images depicting the particle surfaces of ponded ash and fly ash are given in Fig. 4. As can be observed, many fly ash particles are in the porous structure of ponded ash. In addition, many fly ash particles can be seen (i.e., spherical shapes) from the particle surfaces of ponded ash (SEM image) shown in Fig. 4.

Experimental Methods

In the experimental program, numerous CLSM mixtures were made and are described in Table 4. In this work, four CLSM groups were produced, named WB-C, WB-CB, WS-C, and WS-CB, corresponding to the ratios of water to binder (W:B) (i.e., changing amount of binder content), water to solid (W:S) (i.e., changing amount of water content), and two binder types including cement and cementless binder. In order to be used as a grout in geothermal systems, the flowability (ability of grout to flow easily into boreholes), bleeding (property that controls the loss of grout depth in boreholes), compressive strength (reflecting the bearing capacity of grout), environmental impacts (causing the potential risk of water pollution), and thermal conductivity (reflecting the heat-transfer capacity of grout) are the most important, and they were the focus of this study. However, the durability properties (freeze-thaw) were not evaluated. With regards to mixing sequence, the aggregates and binders were first dry-mixed for 5 min to ensure that all mixtures were in homogeneity. The designed amount of water was then added and mixed for at least 10 min. The selection of mixing time for the sample preparation was based on Chapter 6 (“Mixing, transporting, and placing”) of ACI 229R (ACI 1999), which states that a minimum of 15 min (in total) is required to produce homogeneous CLSM slurry. In this study, CLSM consists of fine aggregate (not including coarse aggregate), binders, and a very high amount of water for controlling the flowability and low strength. Therefore, after 5 min of dry-mixing and at least 10 min of being mixed with water, the fresh mixture could be considered to be in homogeneity. Mixing of the mixture was performed by a 10-L mixer in the laboratory. The properties of the mixture such as bleeding, flowability, fresh density, setting time, and compressive strength were tested in accordance with applicable ASTM standards, namely ASTM C940 (ASTM 2016), ASTM D6103 (ASTM 2017b), ASTM D6023 (ASTM 2007), ASTM C403 (ASTM 2008), and ASTM D4832 (ASTM 2002), respectively.

Regarding the environmental impacts of the CLSM mixtures, corrosivity evidenced by pH values and the concentration of heavy metals were performed with the leachate of all CLSM specimens. The pH value of leachate water from CLSM mixtures was measured to use as an evidence of corrosivity. As reported by CFR (2003) and Kim et al. (2016), a solid waste that has a pH value either below 2.0

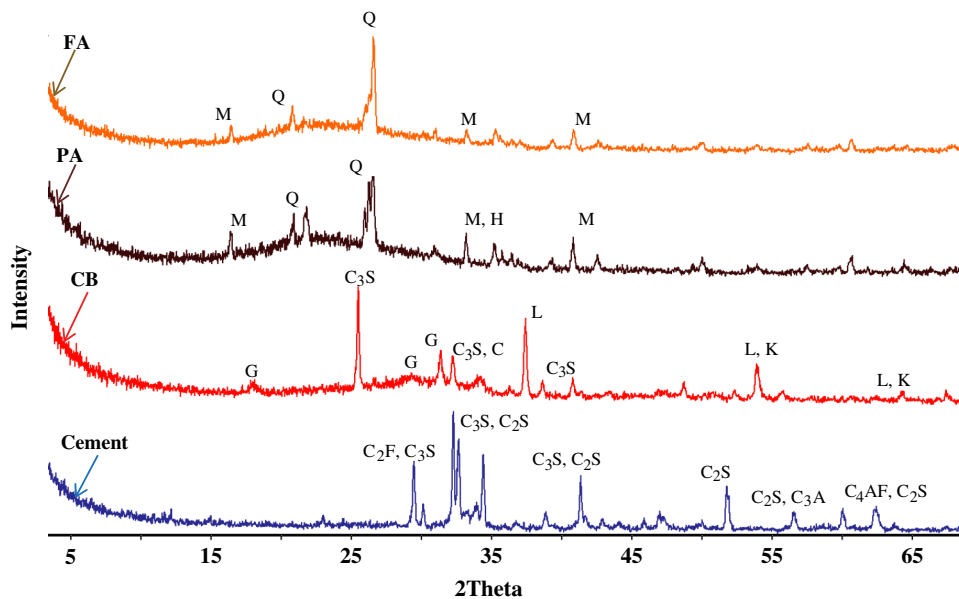


Fig. 3. XRD spectra of ponded ash, fly ash, cement, and CB. Q = quartz; M = mullite; H = hematite; L = lime (free CaO); K = kaolinite; C₃S = alite; C₂S = belite; C₃A = tricalcium aluminate; C₄AF = celite; C₂F = brownmillerite; G = gypsum; and C = calcite.

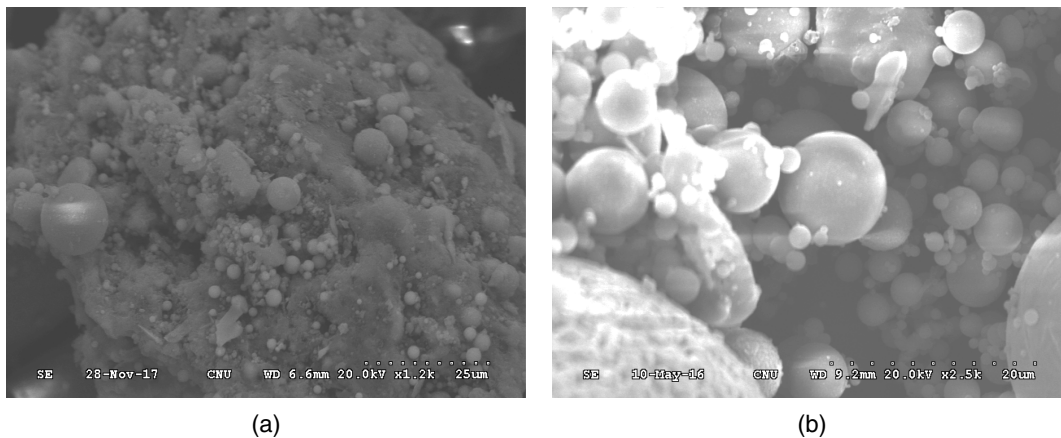


Fig. 4. SEM images of particle surfaces of (a) ponded ash; and (b) fly ash.

Table 4. Total mix proportions of various CLSM mixtures

Mix code	Ratio		Unit weight (kg/m ³)				Fresh density (kg/m ³)	Cement
	W:B	W:S	PA	Binders				
				Cement	CB	Fly ash		
WB1C	1.2	—	1,067.03	79.52	0.00	280.74	1,857.97	4.28
WB2C	1.15	—	1,070.63	93.91	0.00	281.74	1,878.29	5.00
WB3C	1.1	—	1,065.02	107.48	0.00	280.28	1,882.33	5.71
WB1CB	1.2	—	1,066.56	0.00	79.49	280.62	1,857.15	0.00
WB2CB	1.15	—	1,069.85	0.00	93.85	281.54	1,876.93	0.00
WB3CB	1.1	—	1,063.00	0.00	107.28	279.75	1,878.76	0.00
WS1C	—	0.27	1,097.24	96.29	0.00	288.70	1,880.76	5.12
WS2C	—	0.3	1,070.63	93.91	0.00	281.74	1,878.29	5.00
WS3C	—	0.33	1,044.02	91.62	0.00	274.68	1,873.70	4.89
WS1CB	—	0.27	1,096.98	0.00	96.27	288.63	1,880.32	0.00
WS2CB	—	0.3	1,069.85	0.00	93.85	281.54	1,876.93	0.00
WS3CB	—	0.33	1,043.99	0.00	91.62	274.67	1,873.63	0.00

Note: WB-C = water to binder (CLSM made with cement); WB-CB = water to binder (CLSM made with cementless binder); WS-C = water to solid (CLSM made with cement); WS-CB = water to solid (CLSM made with cementless binder); and PA = ponded ash.

or above 12.5 can be corrosive. In general, corrosive materials can release toxic metals and matter directly to the environment or even harm human health. In order to evaluate heavy-metal existence in the proposed CLSM, all of the prepared CLSM mixtures were tested according to the toxicity characteristic leaching procedure of USEPA 1311 (USEPA 1997). The CLSM specimens were crushed to ensure every particle was smaller than 9.52 mm. An extraction fluid following USEPA 1311 was prepared and then employed for the test. After that, the specimen was stirred with the prepared extraction fluid (20 times the weight of the crushed CLSM) for 18 h. Vacuum filtration (0.6 μm) was then used to filter and get leaching fluid from the separation process. Finally, leaching fluid from the vacuum filtration was ready for analysis of toxicity characteristic leaching procedure (TCLP) metals by using inductively coupled plasma-atomic emission spectrometry (ICPMS).

The final test in the experimental program was the thermal conductivity test, which was carried out coincidentally with the unconfined compressive strength (UCS) test conforming to ASTM D5334 (ASTM 2014). At the curing age of 28 days, the thermal conductivity tests were performed on the saturated CLSM specimens. In general, high thermal conductivity is required for the effective heat-transfer ability of CLSM. As stated in ASTM D5334, a thermal needle probe was used in the thermal conductivity test. It contains a temperature measuring element and a heating element. During the test, this needle is penetrated into the specimen. Thermal conductivity λ can be obtained using Eq. (1)

$$\lambda = \frac{Q}{4\pi(T_2 - T_1)} \ln(t_2/t_1) \quad (1)$$

where λ = thermal conductivity [$\text{W}/(\text{m} \cdot \text{K})$]; $Q = I^2(R/L)$ is heat input (W/m), where R is total resistance of heater wire of thermal needle (Ω), I is current of heater wire in thermal needle (A), and L is thermal needle length (m); t_1 = Time 1 (s); t_2 = Time 2 (s); and T_1 and T_2 = temperature (K) at times t_1 and t_2 .

Results and Analysis

General Properties of CLSM

Flowability

Flowability is one of the most important properties of CLSM because it controls the self-leveling ability. The total amount of water

in CLSM mixtures usually control the flowability. In general, good flowability can be obtained in CLSM mixtures containing high water content. However, adding a large amount of water to CLSM can be a reason for an increase in bleeding, strength reduction, and even aggregate segregation. Therefore, the optimum water content should be well-designed for mixing proportion to acquire the best engineering performance of CLSM. Fig. 5 shows all flowability test results of CLSM mixtures. As a result, flowability values varied in the range of 230–300 mm, which expectedly conformed to the good flowability grade reported in ACI 229R (ACI 1999). Moreover, a relationship between flowability and both ratios (W:B and W:S) was observed. The W:B values corresponding to Fig. 5(b) are 1.0 (W:S = 0.27), 1.15 (W:S = 0.30), and 1.27 (W:S = 0.33).

Flowability increased with an increase of the W:S ratio. In particular, when the W:S was 0.27, the flowability reached the minimum requirement of 200 mm specified for general CLSM. With an increase in W:S to 0.3 or 0.33, the flowability increased correspondingly, regardless of binders. An increase in water amount further tended to diminish the viscosity of the CLSM mixtures and finally led an increase in flowability. Similarly, flowability also increased as W:B increased. Because CLSM mixtures were prepared with fixed amounts of water and aggregate, increasing amounts of binders caused a need for more mixing water for the hydration reaction. However, the influence on flowability of the W:S ratio was more slightly pronounced than that of the W:B ratio.

In this study, W:B represents the ratio of water to binder (i.e., amount of binder content is changed and amount of water is fixed) whereas W:S corresponds to the ratio of water to solid (i.e., amount of water is varied and amount of binder is fixed). Flowability of CLSM is mainly controlled by the water amount in this mixture [ACI 229R (ACI 1999)]. Therefore, the influence of W:S is higher than that of W:B on the flowability. In addition, it was observed that regardless of the both ratios (W:B and W:S), flowability values of CLSM mixtures incorporated with CB were slightly higher than those incorporated with cement. This is due to the presence of slag (a workability improver) in cementless binder (Raghavendra and Udayashankar 2013; Lachemi et al. 2010; Sheen et al. 2013).

Bleeding

Water, which is used for flowability of CLSM mixtures, is commonly released to the surface as bleed water or sometimes absorbed by surrounding soil [ACI 229 (ACI 1999)]. Fig. 6 shows the bleeding values of all CLSM mixtures in this study, ranging from

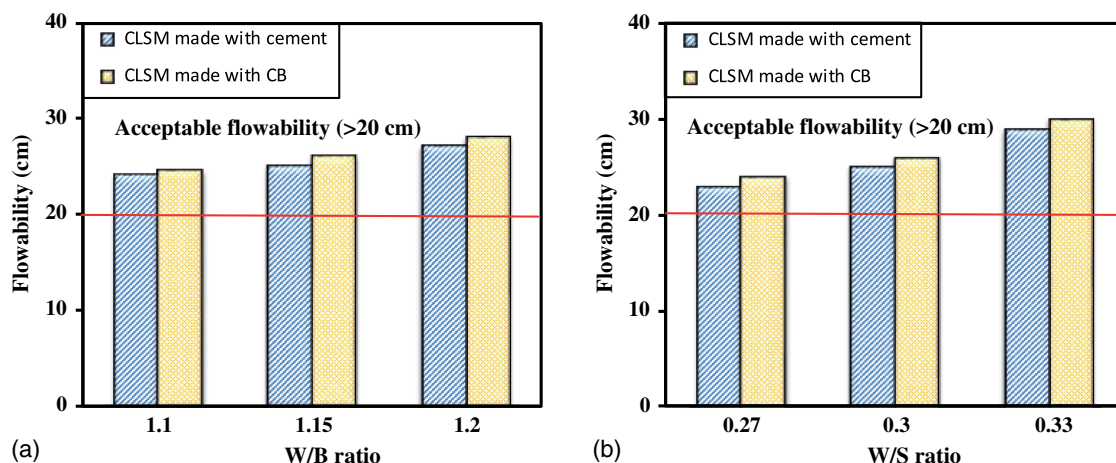


Fig. 5. Flowability of the various CLSM mixtures with respect to (a) W:B; and (b) W:S.

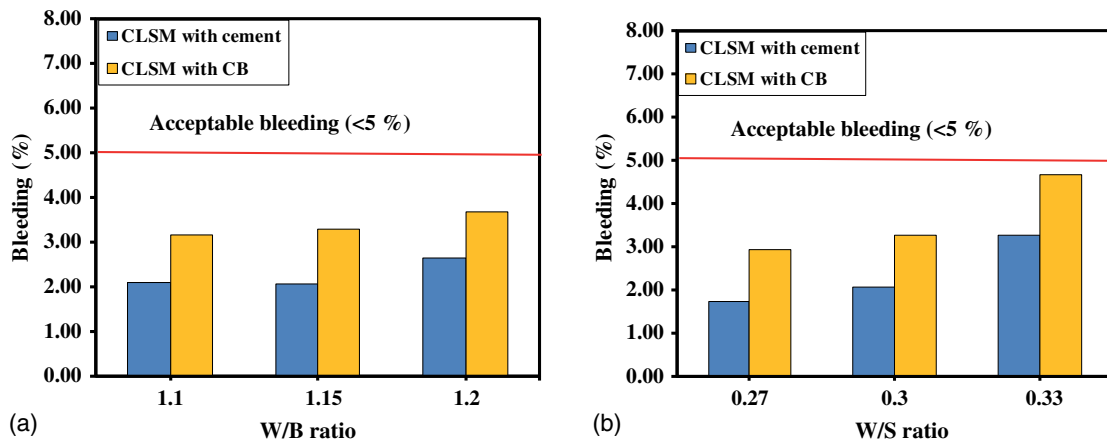


Fig. 6. Bleeding with respect to (a) W/B; and (b) W/S.

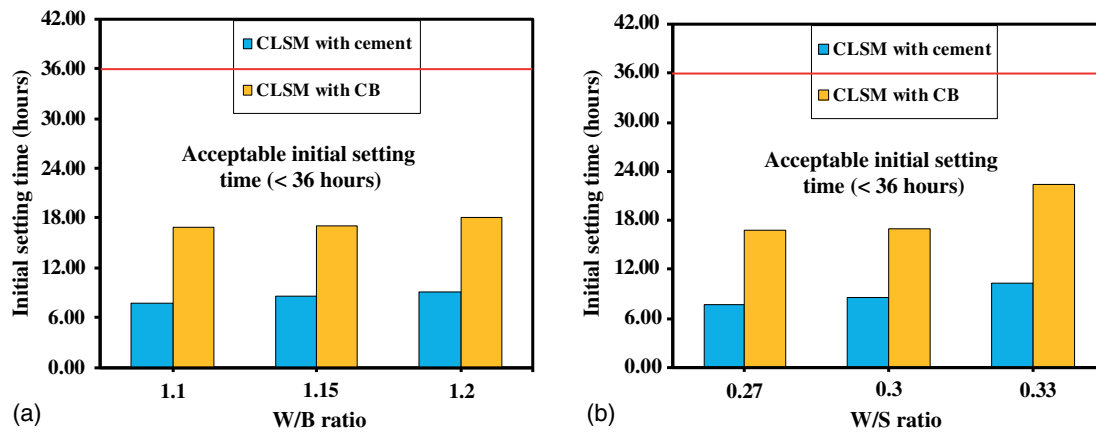


Fig. 7. Initial setting with respect to (a) W/B; and (b) W/S.

1.72% to 4.68%. These values were in the desirable range of CLSM (less than 5% by volume at 2 h) (Gabr and Bowders 2000; Yan et al. 2014) and more stable than those of previous CLSM mixtures, which were also produced using industrial wastes, as stated by Razak et al. (2009) (1.2%–7.2%) and Tikalsky et al. (2004) (0%–8.73%). In addition, bleeding is affected by W:S and W:B ratios, as exhibited in Fig. 6. Bleeding increased with both W:S and W:B ratios. When W:S increased, the amount of water added to CLSM mixtures is more than that required for the hydration process in mixtures. With an increase in W:B (i.e., amount of binder reduced), bleeding increased due to a reduction of the absorption of excess water by binders particles. Similarly, higher flowability values of CLSM mixtures incorporated with CB were observed relative to those incorporated with cement, regardless of W:B and W:S, due to the high amount of slag in cementless binder.

Initial Setting Time

Fig. 7 shows all initial setting time values in the experimental program. As is well-known, CLSM can be used in various applications in the field such as backfills, void fills, structural fills, utility and pipe bedding, or even bridge approach applications. For these applications, the setting time required for CLSM is considered to ensure that after that certain time, a person can walk on it or light construction equipment is able to move across the surface of CLSM without any apparent damage [ACI 229R (ACI 1999)]. As a result, initial setting times varied in the range of 7.65–22.47 h. They were

all shorter than 36 hours, which is the maximum requirement time for general CLSM (Kuo et al. 2013). In addition, an increase in W:B and W:S ratios tended to prolong the initial setting times of CLSM mixtures. The initial setting times of WB3C (W:B = 1.1), WB3CB (W:B = 1.1), WS1C (W:S = 0.27), and WS1CB (W:S = 0.27) were 7.82, 16.83, 7.65, and 16.79 h, respectively. These times were delayed by 16.24% (9.09 h) and 7.37% (18.07 h) at a W:B ratio of 1.2 and by 34.9% (10.32 h) and 33.83% (22.47 h) at a W:S ratio of 0.33. Increasing amount of water and decreasing amount of binder in of CLSM mixtures apparently caused a postponement of the hydration process, which led to the longer initial setting times. Furthermore, CLSM mixtures made with cement had shorter setting times than those made with cementless binder, regardless of W:B and W:S ratios. The longer setting time of CB compared with cement is due to the presence of slag (a pozzolanic material with weak hydraulic properties) (Muhmood et al. 2009). Overall, all of CLSM mixtures in this study still met the setting time requirement of CLSM.

Unconfined Compressive Strength of CLSM Mixtures

UCS (in average) of all proposed CLSM mixtures are shown in Fig. 8. With the hydration process of the cementitious mixtures in binders, compressive strengths of all prepared CLSM mixtures increased with respect to curing ages. The 3-day and 7-day strengths ranged from 0.15 to 1.0 MPa and 0.28 to 1.31 MPa, respectively. The 28-day strengths of all CLSM mixtures varied in the range

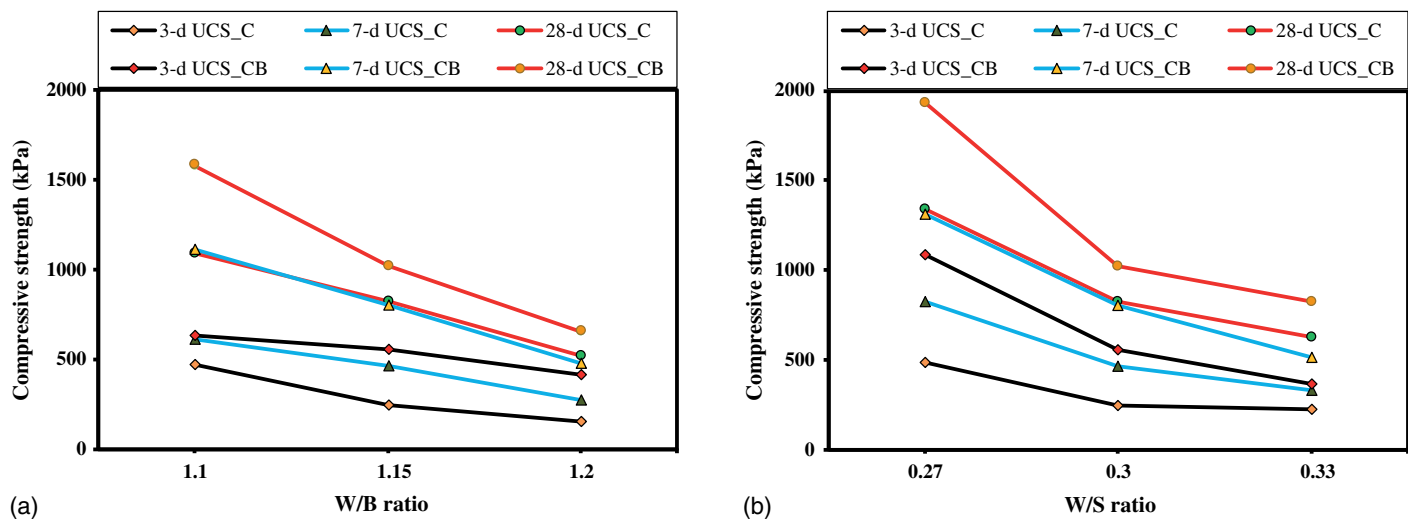


Fig. 8. UCS with respect to (a) W:B; and (b) W:S.

of 0.52–1.94 MPa, meeting the targeted strengths for future re-excitation (less than 2.1 MPa) [ACI 229R (ACI 1999)]. It can be observed that UCS of each CLSM mixtures varied as a function of W:B and W:S ratios. The values of UCS decreased with increases in both ratios (W:B and W:S). However, there was larger curing effect on compressive strength (i.e., strength development) at smaller W:B and W:S ratios, as shown in Fig. 8. The compressive strength of CLSM, known as a very-high-water-content mixture, is significantly affected by the total amount of cement or water used in this mixture (i.e., the larger the cement or lower the water amount used in this mixture, the more strength development is observed). In this study, the smaller W:B ratio mixture represents for CLSM containing the higher amount of cement, whereas the smaller W:S ratio mixtures are representative of that incorporating lower water amount. In this sense, it is reasonable to find that the more strength development (larger curing effect on compressive strength) at the smaller W:B and W:S ratios.

Fig. 8 represents the unconfined compressive strength of various CLSM mixtures with respect to curing time. It can be seen clearly that the compressive strength of all CLSM mixtures made with cementless binder showed slightly higher values than those of CLSM made with cement in every curing age. The reaction of pozzolanic material (fly ash), which is activated by lime in cementless binder, is expected to generate calcium silicate hydrate gel (CSH). Lime releases OH⁻ ions in the presence of water to supply the high alkaline environment in the mixture. Under this condition, the surface of fly ash is hydrolyzed and finally, tSi, Al (from fly ash), and Ca (from lime in CB) species react with each other to form CSH gel (Lee et al. 2013). In addition, the mechanism of strength formation of CLSM made with cementless binder is expected by the chemical reactions of pozzolanic materials. In cementless binder, SO₃²⁻ ion released from gypsum could react with Al³⁺ (from slag) or Al³⁺ (from fly ash), and calcium oxide in lime to form ettringites (Mun et al. 2007). Eventually, the pores in the specimens are then filled up by both CSH and ettringites, thereby hardening the specimens (as depicted in the SEM results).

Microstructural Analysis

X-Ray Diffraction Analysis

The 28-day XRD patterns of CLSM mixtures made with cement and cementless binder are displayed in Fig. 9. A series of chemical

compounds or peaks such as quartz (Q), ettringite (E), calcium silicate hydrate (CSH), calcium aluminate silicate hydrate (CASH), portlandite (CH), calcite (C), and dehydrate gypsum (G) were observed. In the CLSM mixture made with cement, one can observe a strong peak of quartz (26°) 2θ (i.e., existed as mineral itself, probably originated from pond ash) and medium peaks of CSH and CH (29°) 2θ [i.e., in the presence of water, the compound C₃S in both cement formed products of hydration via the process 2C₃S + 6H → C₃S₂H₃ + 3Ca(OH)₂]. Besides, due to the presence of fly ash in CLSM mixtures, other weak peaks of CSH also were found because the hump of silica-aluminous glass in fly ash was dissolved under the alkaline environment to form CSH gels (12°, 20°, 35°, and 48°) and CH (23°) through polymerization (Lee et al. 2013; Yan et al. 1998). Similarly, due to the presence of compound C₃S in cementless binder (as shown in XRD spectra of the original cementless binder), the identical hydration products of CSH and CH were also observed in the CLSM mixture made with cementless binder.

However, different from the CLSM mixture made with cement, there were various ettringite peaks (9°, 16°, 23°, 35°, and 42°) observed in the XRD result of the CLSM mixture made with cementless binder. In addition, a low peak of gypsum (12°) existing as the mineral itself was also observed from the XRD results of CLSM mixture made with cementless binder. The presence of gypsum and calcium oxide (i.e., in slag and lime) was believed to produce ettringites in the CLSM mixture. It encouraged release of greater amounts of sulfate ions, which reacted with alumina phase of fly ash or slag (Plowman 1984; Min et al. 2008) to enhance more formation of ettringite, as evidenced from SEM results.

Scanning Electron Micrograph Analysis

Figs. 10 and 11 show the 3-day and 28-day SEM results of CLSM mixtures made with cement and cementless binder, respectively. It can be observed that fly ash particles were wrapped by bonding gels, which were results of the hydration process of fly ash. It was completely different from the SEM result of raw material fly ash with smooth surfaces [Fig. 11(a)]. However, the characteristics of these bonding gels were different with respect to curing ages or binders used. At the age of 3 days, apart from a small amount of calcium silicate hydrate formed by cement or cementless binder, the slight surface dissolution on fly ash particles can be observed due to the hydration reaction of pozzolanic materials. As shown,

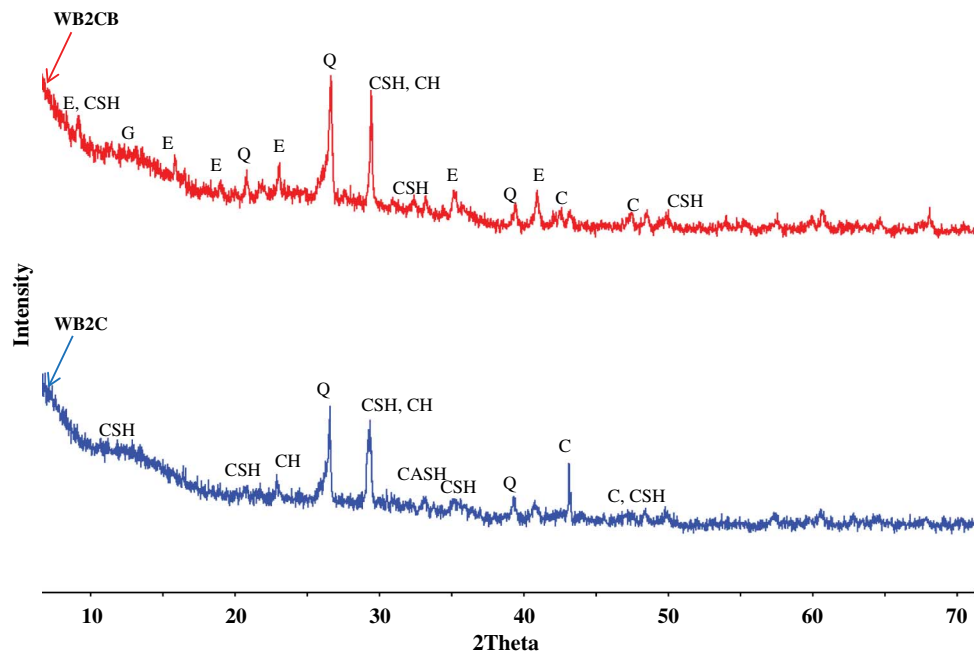


Fig. 9. XRD spectra of the representative CLSM hardened mixtures made with cement and cementless binder. CSH = calcium silicate hydrate; E = ettringite; CASH = calcium aluminum silicate hydrate; Q = quartz; C = calcite; and G = dehydrate gypsum.



Fig. 10. SEM image of CLSM mixture made with cement.

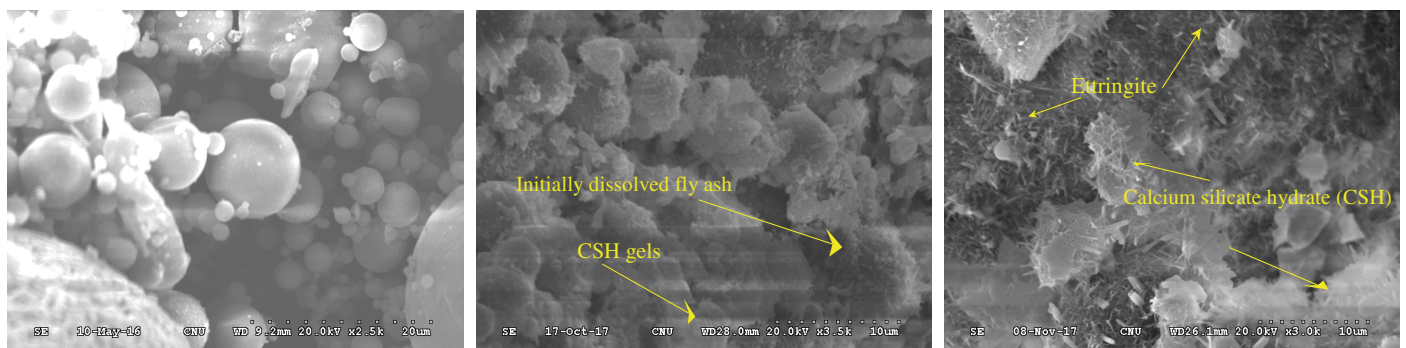


Fig. 11. SEM image of CLSM mixture made with cementless binder compared with original fly ash.

there were thin bonding gels wrapping around fly ash particles. However, most of the fly ash particles still retained their spherical shapes, and some fly ash particles retained even their smooth surfaces, which indicated that the hydration reaction of fly ash had

rarely developed at the early ages of curing (Ranganath et al. 1998). At the age of 28 days, there was evidence of further hydration with the pronounced formation of CSH Type I (tobermorite) in amorphous shape (CLSM mixture made with cement) and ettringite with

Table 5. pH values of various CLSM

Mix identifier	Bleeding (%)	Bleed water	pH		
			Leachate water		
			7 days	14 days	28 days
WB1C	2.63	11.92	9.94	10.62	10.96
WB2C	2.062	12.08	10.03	10.74	11.13
WB3C	2.08	12.24	10.11	10.81	11.28
WB1CB	3.684	11.82	9.08	10.0	10.28
WB2CB	3.271	11.96	9.22	10.09	10.4
WB3CB	3.16	12.05	9.37	10.2	10.54
WS1C	1.724	12.13	10.15	10.82	11.19
WS2C	2.062	12.08	10.03	10.74	11.13
WS3C	3.257	12.00	9.96	10.6	11.02
WS1CB	2.914	12.00	9.36	10.17	10.51
WS2CB	3.271	11.96	9.22	10.09	10.40
WS3CB	4.678	11.87	9.0	10.0	10.32

very dense and thick needle-shaped structures (CLSM mixture made with cementless binder). These findings agreed well with those from XRD analysis. The large enhancement ettringite in CLSM made with cementless binder led to an increase in the unconfined compressive strength, slightly larger than that of CLSM made with cement, as experimentally observed. Voids in the specimen were filled with hydrated products, both CSH and ettringite, to significantly improve the strength of CSLM made with cementless binder.

Environmental Impacts of All CLSM Mixtures in the Experimental Program

Concerning the environmental impacts of CLSM, corrosivity as evidenced by pH values and the concentration of heavy metals were performed with the leachate of all CLSM specimens. The pH values of the CLSM mixtures were measured from bleed and leachate water collected from various CLSM specimens and are tabulated in Table 5. The pH values of leachate water were measured at the age of 7, 14, 21, and 28 days after sampling. The pH values of leachate and bleed water were in the ranges of 9.0–11.28 and 11.82–12.24, respectively. The bleed and leachate water were totally alkaline due to the hydroxide released from the hydration process in CLSM mixtures. However, the range of pH values was still smaller than 12.5 (the limitation of corrosivity for the alkaline specimens). Therefore, all CLSM mixtures possessed sufficient resistance to corrosivity (CFR 2003; Razak et al. 2009; Tikalsky et al. 2004; Kim et al. 2016). In addition, it can be observed from all proposed CLSM mixtures in Table 5 that bleed water has higher pH values than leachate water. This agrees well with the results presented by Razak et al. (2009) and Kim et al. (2016). Moreover, the pH values of CLSM mixtures (bleed and leachate water) incorporated with cementless binder were fairly lower than those of mixtures that incorporated cement.

In addition to corrosivity, heavy metals in CLSM also should be considered as an aspect of the environmental impacts because, as reported in ACI 229R, CLSMs are usually applied as backfill, structural fill, or void fill materials that contact directly with the surface or groundwater. These conditions could be caused a potential risk of water pollution through leaching such heavy metals into groundwater. The most common contaminants of heavy metals are arsenic (As), cadmium (Cd), chromium (Cr), and lead (Pb) as reported in *Treatment Standard for Hazardous Wastes* (CFR 2003). The test results collected from all CLSM specimens are

Table 6. Results of leachable substances in leachate of various CLSMs

Mix identifier	Concentration (mg/L)			
	As	Cd	Pb	Cr
WB1C	0.21	0.03	0.28	0.54
WB2C	0.17	0.03	0.2	0.5
WB3C	0.06	<0.01	0.01	0.34
WB1CB	0.08	<0.01	0.01	0.29
WB2CB	0.09	<0.01	0.01	0.3
WB3CB	0.08	0.01	0.01	0.16
WS1C	0.09	0.01	0.01	0.17
WS2C	0.17	0.03	0.2	0.5
WS3C	0.07	0.01	0.01	0.18
WS1CB	0.06	0.01	0.01	0.19
WS2CB	0.09	<0.01	0.01	0.3
WS3CB	0.06	0.01	0.02	0.18
CFR 268.40 limits	5	1	5	5

Source: Data from USEPA (1997).

listed in Table 6. As a result, the concentrations of all elements including As, Cd, Cr, and Pb satisfied the required specifications stated in CFR (2003). Therefore, the hardened CLSM specimens were classified as nonhazardous materials.

Thermal Conductivity

For every material, the thermal conductivity is defined as the quantity of heat perpendicularly transmitted through a unit thickness to a unit area surface (due to a unit temperature gradient under given conditions) (Sengul et al. 2011). In this study, thermal conductivity testing conforming to ASTM D5334 was performed to evaluate the feasibility of coal ash-based CLSM used as a thermal grout filled in boreholes of geothermal systems. Generally, high thermal conductivity is required for the effective heat transfer ability of CLSM. Fig. 12 shows the thermal conductivity (i.e., thermal needle factor taken into account) with respect to W:S and W:B ratios for the fully saturated CLSM specimens obtained in the present investigation, coupled with the data from M. L. Allan [US Patent No. 6,251,179 B1 (2001)]. As a result, the thermal conductivity values of all proposed CLSM mixtures ranged from 1.04 to 1.47 W/mK, sufficiently higher than those of conventional grouts (e.g., net cement grout and high solids bentonite grout).

In addition, it can be observed that thermal conductivity slightly decreased with an increase in both ratios of W:B and W:S. When the ratios of W:B and W:S were 1.1 and 0.27, the maximum thermal conductivity values were observed, similar to those of thermally enhanced bentonite grout [M. L. Allan, US Patent No. 6,251,179 B1 (2001)]. When these ratios increased (i.e., water amount increasing and binder amount decreasing), the thermal conductivity values slightly reduced because the increasing amount of water and decreasing amount of binder apparently left pores in the hardened CLSM mixtures. In others words, CLSM mixtures with high W:B and W:S ratios would have greater porosity and lower thermal conductivity than those with low such ratios. However, these thermal conductivity values are still likely higher than those of conventional grouts (e.g., net cement grout and high solids bentonite grout). In addition, the thermal conductivity of controlled low-strength material made with cementless binder was satisfactory in a comparison with that of conventional grouts. This finding is important when the CLSMs made with cementless binder are considered to be used for an alternative grout for borehole heat exchangers.

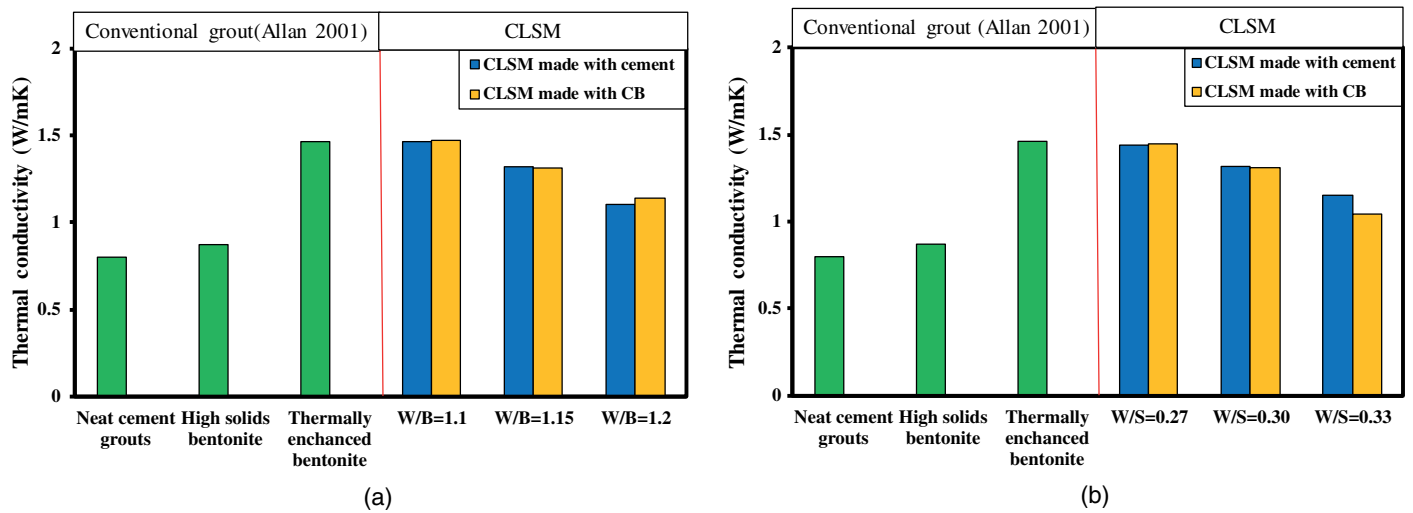


Fig. 12. Thermal conductivity of CLSM in comparison with conventional grouts with respect to (a) W/B; and (b) W/S.

Conclusions

Conventionally, CLSM consists of standard materials such as cement, natural sand as an aggregate, and binder. In this study, CLSM was newly designed for the feasible usage as a thermal grout in borehole heat exchangers. In particular, pond ash, a by-product from a thermal power plant, was recycled to replace natural sand. In addition, a cementless binder, which is a cementitious mixture composed of fly ash, lime, and gypsum, was employed for the production of CLSM. As a result, all of the prepared CLSM mixtures performed similarly well and met to the requirements of ACI 229R regarding all engineering properties, environmental impacts, and the key parameter, thermal conductivity. Furthermore, the use of cementless binder could lead to improving the flowability, which is a key aspect of the performance of CLSM in terms of workability of thermal grout for borehole heat exchangers. Eventually, owing to a good flowability and a higher thermal conductivity than conventional grouts, the CLSMs made with cementless binder could be used as a thermal grout for borehole heat exchangers.

However, the properties of the proposed CLSM would be affected by various factors in the real field. Therefore, in order to ensure the efficiency of the proposed CLSM grout for borehole heat exchangers in the field, a large-scale field test is expected to be performed in future work.

Acknowledgments

This work was supported by a National Research Foundation of Korea (NRF) grant funded by the Korea government (MSIT) (Grant No. NRF-2018R1A2B6007567).

References

- ACI (American Concrete Institute). 1999. *Controlled low strength materials*. ACI 229R-99. Farmington Hill, MI: ACI.
- Allan, M. L. 1997. *Thermal conductivity of cementitious grouts for geothermal heat pumps*. FY 97 Progress Rep. BNL 65 129. Upton, NY: Brookhaven National Laboratory.
- Allan, M. L., and S. P. Kavanaugh. 1999. "Thermal conductivity of cementitious grouts and impact on heat exchanger length design for ground source heat pumps." *HVAC&R Res.* 5 (2): 85–96. <https://doi.org/10.1080/10789669.1999.10391226>.
- Alrtime, A. A., M. Rouainia, and D. A. C. Manning. 2013. "Thermal enhancement of PFA-based grout for geothermal heat exchangers" *Appl. Therm. Eng.* 54 (2): 559–564. <https://doi.org/10.1016/j.applthermaleng.2013.02.011>.
- ASTM. 2002. *Standard test method for preparation and testing of Controlled Low Strength Material (CLSM) test cylinders*. ASTM D4832. West Conshohocken, PA: ASTM.
- ASTM. 2004. *Standard specification for Portland cement*. ASTM C150. West Conshohocken, PA: ASTM.
- ASTM. 2007. *Standard test method for density (unit weight), yield, cement content, and air content (gravimetric) of Controlled Low-Strength Material (CLSM)*. ASTM D6023. West Conshohocken, PA: ASTM.
- ASTM. 2008. *Standard test method for time of setting of concrete mixtures by penetration resistance*. ASTM C403. West Conshohocken, PA: ASTM.
- ASTM. 2014. *Standard test method for determination of thermal conductivity of soil and soft rock by thermal needle probe procedure*. ASTM D5334. West Conshohocken, PA: ASTM.
- ASTM. 2016. *Standard test method for expansion and bleeding of freshly mixed grouts for preplaced-aggregate concrete in the laboratory*. ASTM C940. West Conshohocken, PA: ASTM.
- ASTM. 2017a. *Standard practice for classification of soils for engineering purposes (Unified soil classification system)*. ASTM D2487. West Conshohocken, PA: ASTM.
- ASTM. 2017b. *Standard test method for flow consistency of Controlled Low Strength Material (CLSM)*. ASTM D6103. West Conshohocken, PA: ASTM.
- Bera, A. K., A. Ghosh, and A. Ghosh. 2007. "Compaction characteristics of pond ash." *J. Mater. Civ. Eng.* 19 (4): 349–357. [https://doi.org/10.1061/\(ASCE\)0899-1561\(2007\)19:4\(349\)](https://doi.org/10.1061/(ASCE)0899-1561(2007)19:4(349)).
- CFR (Code of Federal Regulations). 2003. *Applicability of treatment standards*. CFR 268.40. Washington, DC: CFR.
- Chantal, M. 2016. "Improvement of thermal conductivity of grout mixture for geothermal heat pump systems." In *Proc., Int. Refrigeration and Air Conditioning Conf.* West Lafayette, IN: Purdue Univ.
- Chittoori, B., A. J. Puppala, and A. Raavi. 2013. "Strength and stiffness characterization of controlled low-strength material using native high-plasticity clay." *J. Mater. Civ. Eng.* 26 (6): 04014007. [https://doi.org/10.1061/\(ASCE\)MT.1943-5533.0000965](https://doi.org/10.1061/(ASCE)MT.1943-5533.0000965).
- Do, T. M., G. O. Kang, N. Vu, and Y. S. Kim. 2018. "Development of a new cementless binder for marine dredged soil stabilization: Strength behavior, hydraulic resistance capacity, microstructural analysis, and environmental impact." *Constr. Build. Mater.* 186: 263–275.
- Do, T. M., Y. S. Kim, and B. C. Ryu. 2015. "Improvement of engineering properties of pond ash based CLSM with cementless binder and artificial aggregates made of bauxite residue." *Int. J. Geo-Eng.* 6 (1): 8–18. <https://doi.org/10.1186/s40703-015-0008-1>.

- Du, L., K. J. Folliard, and D. Trejo. 2002. "Effects of constituent materials and quantities on water demand and compressive strength of controlled low-strength material." *J. Mater. Civ. Eng.* 14 (6): 485–495. [https://doi.org/10.1061/\(ASCE\)0899-1561\(2002\)14:6\(485\)](https://doi.org/10.1061/(ASCE)0899-1561(2002)14:6(485)).
- Eckhart, F. 1991. *Grouting procedures of ground-source heat pump systems*. Tulsa, OK: Ground Source Heat Pump Publications.
- Gabr, M. A., and J. J. Bowders. 2000. "Controlled low-strength material using fly ash and AMD sludge." *J. Hazard Mater.* 76 (2–3): 251–263.
- KEMCO (Korea Energy Management Corporation). 2006. Annual Rep. 2006. Gyeonggi-do, Korea: KEMCO.
- Kim, Y. S., T. M. Do, H. K. Kim, and G. O. Kang. 2016. "Utilization of excavated soil in coal ash-based controlled low-strength material (CLSM)." *Constr. Build. Mater.* 124: 598–605. <https://doi.org/10.1016/j.conbuildmat.2016.07.053>.
- Kuo, W. T., H. Y. Wang, C. Y. Shu, and D. S. Su. 2013. "Engineering properties of controlled low-strength materials containing waste oyster shells." *Constr. Build. Mater.* 46: 128–133. <https://doi.org/10.1016/j.conbuildmat.2013.04.020>.
- Lachemi, M., M. Sahmaran, K. M. A. Hossain, A. Lotfy, and M. Shehata. 2010. "Properties of controlled low-strength materials incorporating cement kiln dust and slag." *Cem. Concr. Compos.* 32 (8): 623–629. <https://doi.org/10.1016/j.cemconcomp.2010.07.011>.
- Lee, D. J. 2012. "A study on the thermal properties of cement-based grout for ground heat exchangers." M.S. thesis, Dept. of Energy and Resources Engineering, Kangwon National Univ.
- Lee, N. K., H. K. Kim, I. S. Park, and H. K. Lee. 2013. "Alkali-activated, cementless, controlled low-strength materials (CLSM) utilizing industrial by-products." *Constr. Build. Mater.* 49: 738–746. <https://doi.org/10.1016/j.conbuildmat.2013.09.002>.
- Min, Y., Q. Jueshi, and P. Ying. 2008. "Activation of fly ash–lime systems using calcined phosphogypsum." *Constr. Build. Mater.* 22 (5): 1004–1008.
- Muhmood, L., S. Vitta, and D. Venkateswaran. 2009. "Cementitious and pozzolanic behavior of electric arc furnace steel slags." *Cem. Concr. Res.* 39 (2): 102–109. <https://doi.org/10.1016/j.cemconres.2008.11.002>.
- Mun, K. J., W. K. Hyoung, C. W. Lee, S. Y. So, and Y. S. Soh. 2007. "Basic properties of non-sintering cement using phosphogypsum and waste lime as activator." *Constr. Build. Mater.* 21: 1342–1350. <https://doi.org/10.1016/j.conbuildmat.2005.12.022>.
- Park, M. S., S. H. Min, J. H. Lim, J. M. Choi, and H. S. Choi. 2011. "Applicability of cement-based grout for ground heat exchanger considering heating-cooling cycles." *Sci. China Technol. Sci.* 54 (7): 1661–1667. <https://doi.org/10.1007/s11431-011-4388-y>.
- Philippopoulos, A. J., and M. L. Berndt. 2001. "Influence of debonding in ground heat exchangers used with geothermal heat pumps." *Geothermics* 30 (5): 527–545. [https://doi.org/10.1016/S0375-6505\(01\)00011-6](https://doi.org/10.1016/S0375-6505(01)00011-6).
- Plowman, C. 1984. "The chemistry of PFA in concrete: A review of current knowledge." In *Proc., 2nd Int. Conf. on Ash Technology and Marketing*, 437–443. Ottawa, ON: ASH Technology Marketing.
- Puppala, A. J., B. Chittoori, and A. Raavi. 2014. "Flowability and density characteristics of controlled low-strength material using native high-plasticity clay." *J. Mater. Civ. Eng.* 27 (1): 06014026. [https://doi.org/10.1061/\(ASCE\)MT.1943-5533.0001127](https://doi.org/10.1061/(ASCE)MT.1943-5533.0001127).
- Raghavendra, T., and B. C. Udayashankar. 2013. "Flow and strength characteristics of CLSM using ground granulated blast furnace slag." *J. Mater. Civ. Eng.* 26 (9): 04014050. [https://doi.org/10.1061/\(ASCE\)MT.1943-5533.0000927](https://doi.org/10.1061/(ASCE)MT.1943-5533.0000927).
- Ranganath, P. V., B. Bhattacharjee, and X. Krishnamoorthy. 1998. "Influence of size fraction of boned ash on its pozzolanic activity." *Cem. Concr. Res.* 28 (5): 749–761. [https://doi.org/10.1016/S0008-8846\(98\)00036-2](https://doi.org/10.1016/S0008-8846(98)00036-2).
- Razak, H. A., S. Naganathan, and S. N. A. Hamid. 2009. "Performance appraisal of industrial waste incineration bottom ash as controlled low strength material." *J. Hazard Mater.* 172 (2): 862–867. <https://doi.org/10.1016/j.jhazmat.2009.07.070>.
- Remund, C. P., and J. T. Lund. 1993. "Thermal enhancement of bentonite grouts for vertical GSHP systems." In Vol. 29 of *Heat pump and refrigeration systems*, edited by K. R. Den Braven and V. Mei, 95–106. New York: ASME.
- Sengul, O., S. Azizi, F. Karaosmanoglu, and M. A. Tasdemir. 2011. "Effect of expanded perlite on the mechanical properties and thermal conductivity of lightweight concrete." *Energy Build.* 43 (2/3): 671–676. <https://doi.org/10.1016/j.enbuild.2010.11.008>.
- Sheen, Y. N., L. H. Zhang, and D. H. Le. 2013. "Engineering properties of soil-based controlled low-strength materials as slag partially substitutes to portland cement." *Constr. Build. Mater.* 48: 822–829. <https://doi.org/10.1016/j.conbuildmat.2013.07.046>.
- Tikal'sky, P. J., H. U. Bahia, A. Deng, and T. Snyder. 2004. *Excess foundry sand characterization and experimental investigation in controlled low-strength material and hot-mixing asphalt*. Final Rep. No. DE-FC36-01ID13794. University Park, PA: Pennsylvania State Univ.
- USEPA. 1997. *Hazardous waste management system, identification and listing of hazardous waste, proposed exclusion*. EPA 1331, 40 CFR Part 261 of Federal Register. Washington, DC: USEPA.
- Xu, Y., and D. D. L. Chung. 2000. "Effect of sand addition on the specific heat and thermal conductivity of cement." *Cem. Concr. Res.* 30 (1): 59–61. [https://doi.org/10.1016/S0008-8846\(99\)00206-9](https://doi.org/10.1016/S0008-8846(99)00206-9).
- Yan, D. Y. S., I. Y. Tang, and I. M. C. Lo. 2014. "Development of controlled low-strength material derived from beneficial reuse of bottom ash and sediment for green construction." *Constr. Build. Mater.* 64: 201–207. <https://doi.org/10.1016/j.conbuildmat.2014.04.087>.
- Yan, P., W. Yang, X. Qin, and Y. You. 1998. "Microstructure and properties of the binder of fly ash-fluorogypsum-portland cement." *Cem. Concr. Res.* 29 (6): 349–354. [https://doi.org/10.1016/S0008-8846\(98\)00214-2](https://doi.org/10.1016/S0008-8846(98)00214-2).